Slower processes of the ultrafast photoisomerization of an azobenzene observed by IR spectroscopy

ARTICLE *in* CHEMICAL PHYSICS · NOVEMBER 2007

Impact Factor: 1.65 · DOI: 10.1016/j.chemphys.2007.06.048

7 AUTHORS, INCLUDING:

Tobias Schrader
Forschungszentrum Jülich
64 PUBLICATIONS **1,042** CITATIONS
SEE PROFILE

Wolfgang J Schreier
Ludwig-Maximilians-University of Munich
45 PUBLICATIONS **818** CITATIONS
SEE PROFILE

Available online at www.sciencedirect.com
ScienceDirect
Chemical Physics 341 (2007) 258–266
Chemical Physics
www.elsevier.com/locate/chemphys

Slower processes of the ultrafast photo-isomerization of an azobenzene observed by IR spectroscopy

F.O. Koller, C. Sobotta, T.E. Schrader, T. Cordes, W.J. Schreier, A. Sieg, P. Gilch *

Department für Physik, Ludwig-Maximilians-Universität, Oettingenstr. 67, D-80538 München, Germany

Received 31 January 2007; accepted 29 June 2007
Available online 13 July 2007

Abstract

The photo-induced *trans–cis* isomerization of the azobenzene derivative 4-nitro-4′-(dimethylamino)azobenzene in polar solution was studied by femtosecond UV/Vis and IR spectroscopy. The UV/Vis experiment reveals two excited state processes; the slower one (1 ps) is the internal conversion to the ground state. The ensuing spectral changes point to vibrational cooling of the nascent *cis* product and the recovered *trans* isomer. Judging from the UV/Vis experiment this ~5 ps process seems to terminate the isomerization. The internal conversion and the cooling also find their manifestation in the IR experiment. In addition slower spectral changes lasting until ~50 ps are detected. These slow IR responses are compared with the behavior of a non-isomerizing analogue, *para*-*N*,*N*-dimethyl-nitroaniline. An origin for this discrepancy is suggested and potential molecular processes causing the slow IR response are discussed.

Keywords: Femtosecond spectroscopy; IR spectroscopy; Photochemistry; Isomerization; Vibrational cooling

1. Introduction

In very simple terms the following picture of an ultrafast photo-isomerization in solution may be drawn (see e.g. Ref. [1]). After photo-excitation an isomerizable molecule experiences an altered electronic potential (see e.g. Ref. [2]). This potential can bring the nuclei of the molecule to regions in conformational space where the energy surfaces of ground and excited states come close to each other or even touch. In these regions internal conversion to the ground state takes place and will go along with a branching into the photo-product channel and the channel which recovers the starting material. After that branching excess energy is re-distributed within the molecule (intramolecular vibrational relaxation) and transferred to the solvent surroundings (vibrational cooling). So the later stages of photo-isomerizations, i.e. those occurring after the return to the ground state surface, should strongly resemble those seen in photochemically inert molecules.

Here, we will put this assumption to an experimental test. We compare the femtosecond UV/Vis and IR signature of a non-isomerizing and an isomerizing molecule. The molecules compared should bear as much similarities as possible. *para*-*N*,*N*-dimethyl-nitroaniline (pDNA, non-isomerizing) and 4-nitro-4′-(dimethylamino)azobenzene (NA, isomerizing) are particularly suited (for their structures see Scheme 1). Due to their dimethylamino- and nitro-substitution both aromatic molecules have a strong push pull character. This results in charge transfer (CT) absorptions and concomitantly a positive solvatochromism (see Ref. [3] for NA and Ref. [4] for *para*-nitroanilines). Most importantly in the present context, both molecules feature similar (short) excited state lifetimes. Excited *para*-nitroanilines are known to undergo rapid internal conversion in polar solution [5–7]. For pDNA in DMSO (the solvent employed in the present study) a time constant for the internal conversion of 0.85 ps has been reported [7]. The process transfers electronic excitation energy of around 25,000 cm^{-1} to vibrational degrees of freedom. Therefore, this and related molecules have widely been used to study vibrational cooling [7–10]. These various

* Corresponding author. Fax: +49 89 2180 9202.
E-mail address: Peter.Gilch@physik.uni-muenchen.de (P. Gilch).

0301-0104/$ - see front matter © 2007 Elsevier B.V. All rights reserved.
doi:10.1016/j.chemphys.2007.06.048

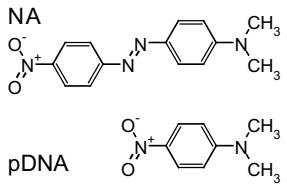

Scheme 1.

studies employing different time resolved techniques agree that cooling in polar solvents takes ~5 ps. For pDNA in DMSO transient absorption experiments in the visible afforded a value of 4.4 ps [7]. NA which undergoes a photo-induced *trans* → *cis* isomerization displays very similar kinetics. In a recent study by our group [11], the photodynamics of NA in toluene has been looked upon by means of femtosecond fluorescence and absorption spectroscopy. The femtosecond fluorescence kinetics had bi-phasic characteristics with time constants of 0.08 and 0.8 ps. These two time constants also show up in the absorption experiment. The longer one could be assigned to the internal conversion to the ground state. Contrary to pDNA the internal conversion not only replenishes the starting material but also goes along with the formation of the *cis* photo-product. Both, the *cis* product and the replenished starting material are vibrationally excited. This results in a characteristic sigmoidal feature in the transient difference spectrum. The decay of this feature, which is roughly equivalent to the cooling time, was ~4 ps for NA in toluene. Another group studied a closely related derivative of NA [12], disperse red 1, and reported cooling times in the range of 3.8–5.3 ps for three different solvents (toluene, acetonitrile, and ethylene glycol). These values nicely match the ones reported for the non-isomerizing pDNA [7]. As far as the spectroscopy in the visible is concerned no differences between pDNA and NA are observed in the dynamics after the internal conversion to the ground state. In the following we will show that pronounced differences are seen in the IR range.

The experiments on NA reported in Ref. [11] have been performed with toluene as a solvent. Since *para*-nitroanilines in non-polar solvents predominantly undergo ultrafast intersystem crossing and not internal conversion [5], toluene is not a suitable solvent for our purpose. Instead, all experiments reported here were performed in DMSO-d_6. Further in all experiments the excitation wavelength was tuned to 400 nm and not as in the previous study to 480 nm (absorption maximum of NA). As will be outlined in the first part of Section 3 changing the solvent and the excitation wavelength has little impact on the spectroscopic signatures of NA in the visible. These signatures will then be compared with those of pDNA. The presentation of the IR experiments begins with a cw characterization of *trans*- and *cis*-NA. This lays the basis for the femtosecond IR experiments on NA. These experiments will reveal slower processes absent in the visible data on NA as well as in the IR data on pDNA. Possible origins of these findings will be addressed in Section 4.

2. Experimental

In both the UV/Vis and the IR femtosecond experiments a 1 kHz Ti:Sa laser/amplifier system served as a light source. Pump and probe pulses in the desired frequency range were generated by non-linear techniques (frequency doubling, NOPA, OPA, and white light generation). The set-up for the UV/Vis absorption experiment is described in Ref. [13], and the IR set-up is detailed in Ref. [10]. The pertinent parameters for the UV/Vis experiment were the following: The laser fundamental (804 nm) was frequency doubled to generate 402 nm pulses with an energy of 500 nJ, which served as pump light. The spot diameter of the pump at the sample location was 150 μm. The white light continuum used as probe light was generated in CaF_2 and covered a spectral range from 350 nm to 640 nm. Pump and probe beams were spatially overlapped at the sample location with a lower diameter for the probe pulse (50 μm) and the polarization at magic angle with respect to the probe light. A time resolution of ~100 fs (FWHM) could be achieved.

In the IR set-up a 407 nm pulse served as the pump. Its energy amounted to 0.7 μJ for pDNA and 3.0 μJ for NA. The diameter of pump beam at the sample location was 150–200 μm. To cover two spectral ranges IR probe pulses centered at 1340 cm^{-1} and 1560 cm^{-1} were employed. They were polarized at an angle of 45° with respect to the pump light. Parallel ($\Delta A_{\parallel}$) and perpendicular ($\Delta A_{\perp}$) signals were simultaneously recorded in multi-channel fashion with two spectrographs. The magic angle signal was calculated according to $\Delta A_m = 1/3\Delta A_{\parallel} + 2/3\Delta A_{\perp}$. A time resolution of ~400 fs (FWHM) was achieved.

NA was synthesized and characterized as described in Ref. [11]. pDNA was purchased from Alfa Aesar (purity >98%) and used as received. Sample solutions in DMSO-d_6 (Sigma–Aldrich, purity 99.8%) were circulated through cells at a speed sufficient to exchange the sample between successive laser shots. The strong background IR absorption of the solvent calls for thin sample films. CaF_2 sample cells with an optical pathlength of 0.1 mm were used. To compensate for the small extinction coefficient in the IR higher sample concentrations (~10 mM) than in the experiment in the visible (~1.0 mM, fused silica windows, pathlength 0.5 mm) were employed.

Steady state IR spectra were recorded by a FTIR spectrometer (Bruker, model IFS 66). IR difference spectra were obtained by illumination of the sample within the spectrometer housing. A cold light lamp (Schott, KLC 2500 LCD) served as a light source. After passing color glass filters (GG400 and BG18 from ITOS, open spectral range 400 nm to about 700 nm) it was directed to the sample by a fiber optic light guide.

Density functional theory (DFT) calculations were performed on the BP86/6-31G** level as implemented in the

Gaussian 98 program package [14]. After optimizing the structures in the *trans* and *cis* conformations IR spectra were calculated for each isomer using the same level of theory. The spectra displayed in Fig. 3c were obtained by convoluting the intensity and frequency output of the calculations with Gaussian line shapes using a constant width (FWHM) of 10 cm^{-1}.

3. Experimental results

3.1. Visible transient absorption spectroscopy

The UV/Vis transient absorption behavior of NA in DMSO-d_6 strongly resembles the one described earlier [11] for NA in toluene: Upon photo-excitation of NA in DMSO-d_6 an instantaneous bleach in the vicinity of the ground state absorption is observed (Fig. 1). On either side of this bleach an induced absorption is found. Within some 100 fs the induced absorption partially decays for short wavelengths and increases for long wavelengths. (In the data representation in Fig. 1 which focuses on slower processes this is difficult to discern. A detailed account of the spectral changes during the first 100 fs is given in Ref. [11].) Later on the induced absorption on either side and the bleach decay with characteristic times of 1–10 ps to a constant offset. Numerical values of the time constants involved were retrieved by a global analysis employing a multi-exponential fit function with proper convolution. At least three exponentials and an offset are required to reproduce the temporal behavior. The time constants determined were to be 0.18, 0.92, and 8.4 ps (errors for all constants are ±15%), the related values for NA in toluene were 0.10, 0.80 and 4.0 ps, respectively [11]. The inspection of the decay associated spectra resulting from the fit (Fig. 1b) yields interesting information: The 0.18 ps time constant marks the decay of the stimulated emission at about 600 nm and of the excited state absorption for $\lambda < 550$ nm. That process does not re-establish the ground state as evidenced by the absence of a negative contribution around 500 nm. The ground state recovers during the next stage with a characteristic time of 0.92 ps. This is indicated by the decaying excited state absorption (350–450 nm and >550 nm) and – more important – the negative signature around 500 nm. It coincides with the ground state spectrum of NA and is thus due to ground state recovery. The 8.4 ps spectrum displays features which are equivalent to a spectral narrowing and blue shift. This is the behavior expected for vibrational cooling in the ground state [15]. The spectral dynamics induced by cooling cannot be exactly represented by the exponential fitting procedure used here and the time constant of 8.4 ps should only be considered as an estimate of the cooling time. A better way to retrieve this cooling time will be presented below. After this cooling period one observes an offset spectrum that matches the feature of the *trans–cis* difference spectrum in toluene. A difference spectrum of NA in DMSO-d_6 could not be recorded. The *cis* form of NA in polar solvents is so short lived [3] that not enough *cis* isomer can be accumulated in a cw-experiment. In toluene the lifetime is prolonged (~70 s [11]) and a steady state difference spectrum is readily recorded. This difference spectrum bears all characteristics of the offset spectrum reported here. When accounting for the solvatochromic shift of the NA absorption when going from toluene to DMSO-d_6 the agreement between the spectra becomes almost quantitative. Thus, as already stated for NA in toluene it looks as if the cooling process on the <10 ps time scale terminates the formation of the *cis*–photo-product and the partial recovery of the initial *trans*-state.

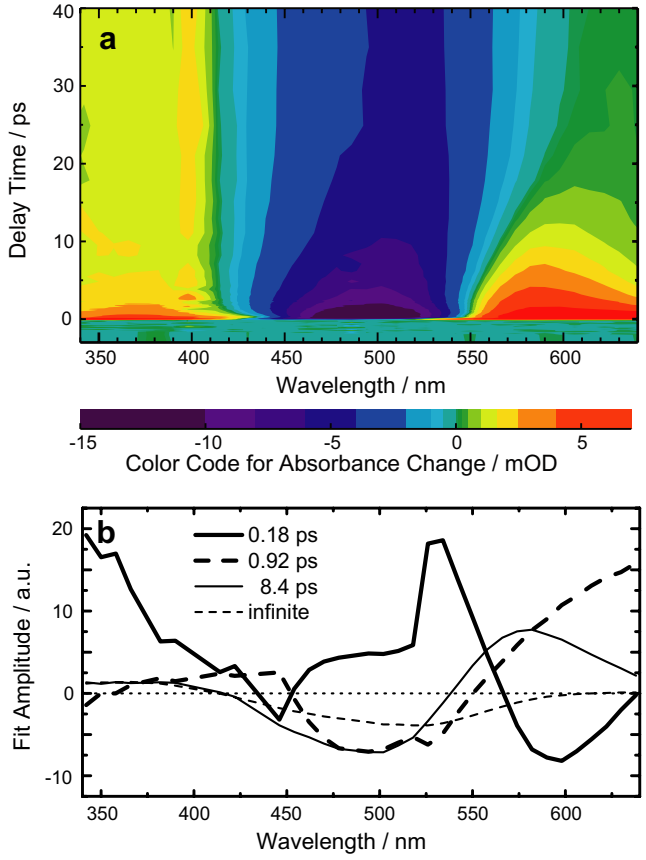

Fig. 1. Absorption changes of NA in DMSO-d_6 induced by femtosecond excitation at 400 nm. (a) gives an overview of the data. The spectra in (b) are derived from a global fit of the transient absorption data. They represent the spectral changes induced by the kinetic processes (decay associated spectra).

As stated above the non-isomerizing molecule pDNA features similar time constants. Our measurements (data not shown) yield time constants of 0.4, 0.9, and 4.9 ps in good agreement with the values reported elsewhere [7]. The shortest time constant has been associated with a process in the excited state and the 0.9 ps component describes the ground state recovery due to rapid internal conversion [7]. This internal conversion time is very close to that determined for NA (0.92 ps). So in either case vibrationally hot ground states are prepared one picosecond after photo-excitation. Cooling times deduced from the exponential

fitting are also very similar. A better way to parameterize this cooling is to monitor the change of the spectrum of the ground state with time. Hot ground states are characterized by broadened and red-shifted absorption spectra (see e.g. Refs. [7,15]). As these states cool, the spectra evolve towards their room temperature shape. This evolution can for instance be described by plotting the mean wavelength of the absorption spectrum λ_{mean} versus time. To determine λ_{mean} the recorded transient *difference* spectra are transformed into *absolute* transient spectra. For this transformation a scaled cw absorption spectrum is added to the time dependent difference spectra. The scaling factor is derived from the ground state bleaching at time zero. This procedure is described in more detail in Ref. [10] albeit for transient IR spectroscopy. It has been applied to the isomerizing NA and the non-isomerizing pDNA (Fig. 2). Almost identical relaxation behaviors of the normalized shifts of the mean wavelengths λ_{mean} are observed. A single exponential description yields relaxation times of 5.5 and 4.7 ps for NA and pDNA, respectively. A bi-exponential treatment yields a somewhat better description, the resulting parameters are compiled in Table 1. The relaxation time of 4.7 ps for pDNA is in excellent agreement with the value reported by Kovalenko et al. (4.38 ps) [7]. The close match of the cooling dynamics of pDNA and NA is in line with the expectation described in Section 1. After the internal conversion to the ground state no differences in the dynamics of isomerizing and non-isomerizing molecules are expected. We will now show that this does not hold true for IR observables.

3.2. IR spectroscopy

3.2.1. Steady state spectroscopy of NA

The steady state absorption and light induced difference spectra are depicted in Fig. 3. The spectral ranges covered in the time resolved measurements are marked by arrows. The most prominent IR resonances in these ranges are (the assignment follows work by Biswas and Umapathy [16]): aromatic C–C stretch vibrations at 1602, 1587, 1517, and 1367 cm^{-1}, a N=N stretch vibration of the azo-group at ~1395 cm^{-1} (visible as a weak shoulder), the symmetric stretch of the nitro-group at 1339 cm^{-1} and a not yet assigned vibration at 1310 cm^{-1}. Furthermore at 1139 cm^{-1} there is the C–N stretch and C–C ring mode and finally at 1105 cm^{-1} another C–C ring mode.

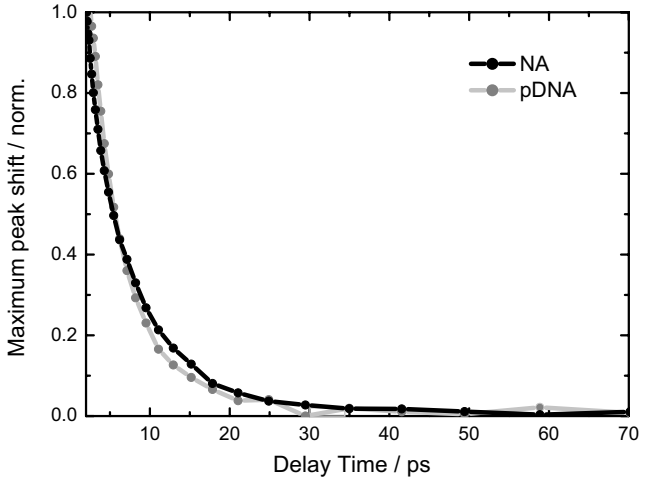

Fig. 2. Temporal evolution of the normalized mean absorption wavelength $\lambda_{mean,n}(t)$ for pDNA (gray line) and NA (black line). The normalized wavelength is given by $\lambda_{mean,n}(t) = (\lambda_{mean}(t) - \lambda_{RT})/(\lambda_{mean}(t = 0) - \lambda_{RT})$, λ_{RT} being the mean absorption wavelength at room temperature.

Table 1
Compiled fitting parameters for the visible transient absorption data

Sample	τ_1	τ_2	τ_3	τ_c	$\tau_{c,1}$	$\tau_{c,2}$
NA	0.18	0.92	8.4	5.5	2.1 (0.44)	8.4 (0.56)
pDNA	0.40	0.90	4.9	4.7	2.7 (0.48)	6.2 (0.52)

The time constants (all in units of picoseconds) τ_i were determined by global fits. For NA the spectra associated with these time constants are plotted in Fig. 1b. The time constant τ_c represents the cooling time derived from single exponential fits of data depicted in Fig. 2. The result of double exponential fits is also given ($\tau_{c,1,2}$). The amplitude of each component is given in parenthesis.

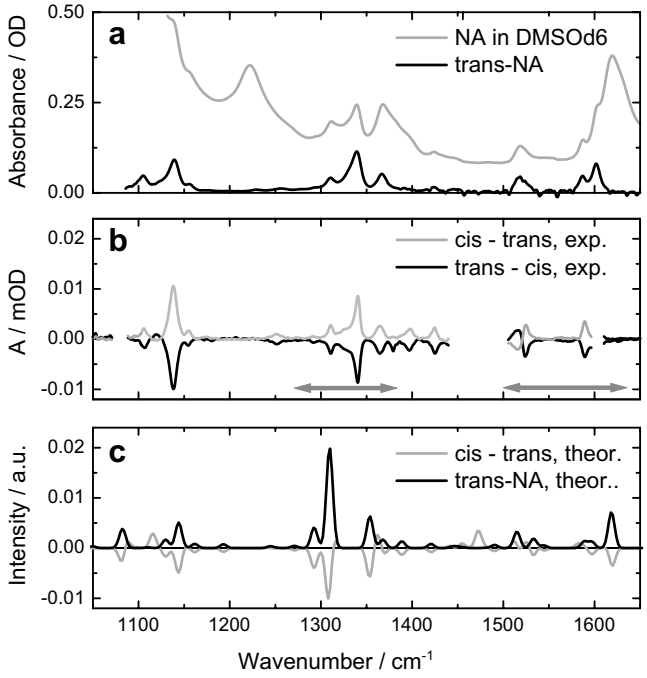

Fig. 3. Steady State IR spectra of NA. (a) IR spectrum of a solution of NA dissolved in DMSO-d_6 (thin gray line) displaying absorption bands of the solvent and the solute and a spectrum of NA where the solvent signature was subtracted (black line). (b) IR absorption changes induced by illumination of a solution of NA in toluene. The black line represents the modulations observed in the photostationary state produced by shining light on a *trans* sample. The gray line stands for the changes detected when starting with a photostationary *cis*/*trans* mixture after complete *trans* recovery. The arrows indicate the spectral ranges covered in the femtosecond IR experiments. Regions that are opaque due to solvent absorptions are not shown. (c) Computed spectrum (BP86/6-31G**) of the *trans*-isomer (black line) and computed *cis–trans* difference spectrum (gray line).

The influence of steady state illumination on the IR spectrum was studied for NA in toluene since (see above) the *cis*-form is too short lived in DMSO-d_6. Two kinds of difference spectra were recorded. Starting with a pure *trans* sample the spectral changes caused by the formation of the photo-stationary state were measured (thick black line in Fig. 3b). Spectral changes with respect to the photo-stationary state were obtained by turning the illumination off (thin gray line in Fig. 3b). That spectrum is – expect for the sign – identical with the first difference spectrum indicating the reversibility of the photo process. The reformation of the initial *trans* isomer proceeds with a time constant of ~70 s. This time constant matches the thermal *cis* → *trans* reaction time determined by UV/Vis spectroscopy [11]. This tells us that the photo-induced IR absorption changes are due to the formation of the *cis*-isomer. The dominant effect of the *cis* formation is a reduction of the IR absorption. Only, for the 1515 cm^{-1} mode a clear sigmoidal difference signature indicative for a frequency shift occurs. The major difference in the IR spectra of *trans* and *cis* lies in the oscillator strength of the vibrational resonance and not in their frequencies.

This observation is reproduced by DFT calculations (BP86/6-31 G**, Fig. 3c). For optimized structures of *trans*-NA and *cis*-NA (depicted in Fig. 7) IR spectra have been calculated. The calculated *trans* spectrum reproduces the general features of the experimental one. The strongest IR resonance is the symmetric NO_2 stretch around 1310 cm^{-1} in either spectrum. Further, the aromatic stretch vibrations around 1600 cm^{-1} or the C–N stretch at ~1100 cm^{-1} are well accounted for by the calculation. In Fig. 3c the calculated *cis–trans* difference spectrum is shown. In agreement with the experimental observations at 1116 cm^{-1} and 1515 cm^{-1} the absorption of the *cis*-isomer exceeds the one of the *trans* isomer. The 1515 cm^{-1} resonance in the *trans* form is due to a CH bending/CN stretch mode localized in the ring near the dimethylamino group. In the *cis* form the CN stretch character of this mode gains importance. The same kind of CN stretch contribution is responsible for an increased absorption of the *cis*-isomer around 1116 cm^{-1}. The *trans*-isomer does not show considerable intensity in this frequency range. But apart from these exceptions the difference spectrum is dominated by signal reductions indicative of lower oscillator strengths in the *cis* isomer. From the measured spectrum this lowering cannot be quantified since the photo-stationary concentration of the *cis* isomer is unknown. The calculations predict a reduction of the oscillator strength of ~30% for the NO_2 stretch vibration.

3.2.2. Femtosecond IR spectroscopy of NA

Femtosecond excitation of NA with 400 nm laser pulses induces pronounced spectral changes in the IR (for an overview see Fig. 4). The common features of this response may be summarized as follows: At negative delay times, i.e. when the IR probe pulse precedes the visible pump pulse, absorption signals due to the perturbed free induction decay [17–19] are present. This effect holds no information on the photo-induced dynamics [18] and it will not be further examined. At time zero intense reductions of the IR absorption of the IR resonances of *trans*-NA assigned above are recorded. In addition, the time zero spectrum contains positive signals (induced absorptions). These broad absorption features are seen in the ranges of 1260–1310 cm^{-1} and 1530–1590 cm^{-1} and decay within ~1 ps.

As these broad bands disappear new induced absorption features clinging to the low frequency wings of the bleaches emerge. With increasing delay time all these bands shift to higher frequencies, thereby partially "eating up" the bleach signals. The spectral shifts occur with a characteristic time constant of ~10 ps. With exception of the weak 1312 cm^{-1} mode, shifts on that time scale are observed for all resonances covered. After roughly 40 ps the spectral positions of the bands have settled. At even later times there is only a change in their amplitudes.

We will highlight these slower changes taking the symmetric NO_2 stretch resonance at 1340 cm^{-1} as an example – but note that a similar behavior is found for the other bands. The transient spectra symbolized by black and gray lines in Fig. 4c describe the dynamics up to 20 ps already discussed above. Of the spectra recorded afterwards the 50 ps spectrum is easy to assign since it comes close to the steady state *cis–trans* difference spectrum in toluene (note that such a difference spectrum cannot be recorded in DMSO-d_6, see above). Thus, this – in the IR – marks the termination of the built-up of the final isomer distribution. The fraction of the *cis*-isomer in this distribution is estimated to be ~10%. This estimate is based on the bleach after 50 ps in relation to the initial bleach. That ratio amounts to 7%. Taking into account that the isomerization reduces the oscillator strength of the NO_2 mode by 30% (see above) one arrives at the given yield. Clearly, that yield is not yet settled after 20 ps since spectral changes occur thereafter. The 20 ps spectrum looks somewhat like a scaled up *cis–trans*-difference spectrum but there are some deviations. The bleach spectrum of the NO_2 mode at 1340 cm^{-1} is sharper and shifted to higher frequencies at 20 ps as compared to the steady state difference spectrum. Furthermore, there are weak induced absorption bands at 1355 and 1320 cm^{-1} that are absent in the steady state difference spectrum. So definitely, there are distinct spectral changes in the IR occurring at delay times when the transient absorption in the visible is already static.

This discrepancy becomes most evident when directly comparing the two experiments. For that comparison the UV/Vis and IR time traces were normalized in the following fashion. Pedestal difference absorptions at $t = 70$ ps (at that time the dynamics are terminated in either experiment) were subtracted to ensure that all time traces decay to the same level. Further, the traces were normalized at $t = 0.25$ ps for excited state dynamics or at $t = 2.0$ ps for the ground state dynamics. At wavelengths/frequencies that predominately probe the electronically excited state (646 nm in UV/Vis, 1260 cm^{-1} in the IR, Fig. 5a) both

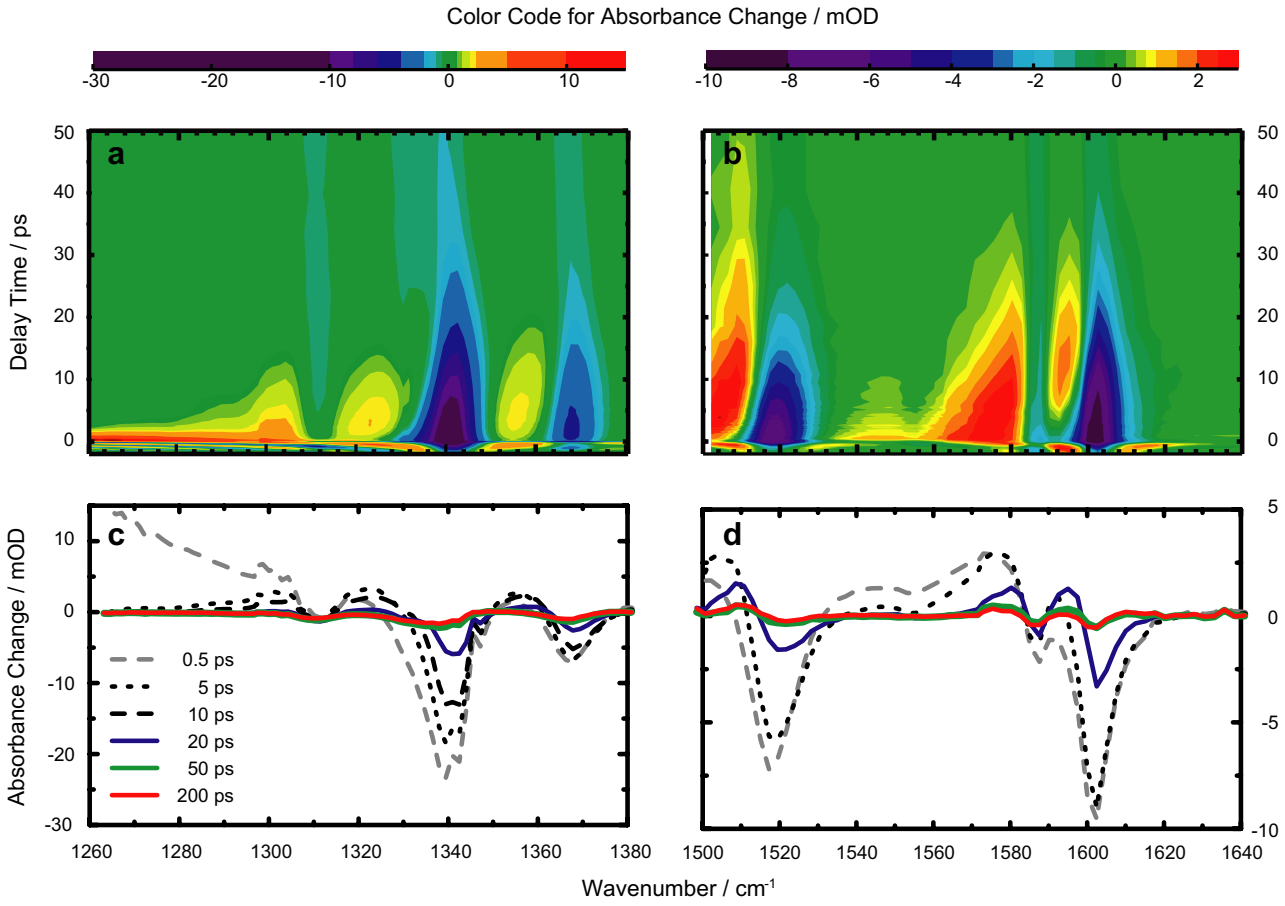

Fig. 4. Changes of the IR absorption upon optical excitation of NA in DMSO-d_6 with femtosecond laser pulses centered at 400 nm. (a) and (b) Contour representation. Negative (absorption bleach, blue coloring) and positive (induced absorption, green to red coloring) changes are observed. Note that the color codings in the two plots differ. (c) and (d) Difference absorption spectra at given delay times. (For interpretation of the references to color in this figure legend, the reader is referred to the web version of this article.)

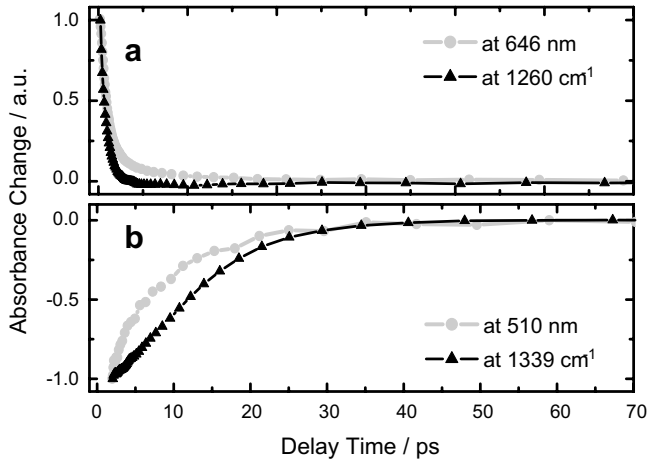

Fig. 5. Comparison of the UV/Vis (gray) and IR (black) transients induced by femtosecond optical excitation of NA in DMSO-d_6. In (a) the detection frequencies were chosen as to focus on the electronically excited state. In (b) emphasis is laid on ground state processes.

experiments feature similar kinetics: The signal around time zero predominately decays with a time constant of ~1 ps. This is due to the depletion of the excited state. In the visible time trace a minor slower contribution caused by ground state cooling is also observed. A different picture emerges when probing the ground state recovery (510 nm in the visible, 1339 cm^{-1} in the IR, Fig. 5b). The transient absorption settles after ~20 ps whereas in the IR the signal continues to evolve until ~50 ps. So by means of IR spectroscopy a slower process – most likely occurring in the electronic ground state – can be observed which does not leave an imprint in the Vis spectroscopy. The question that now arises is whether this slower process is a unique process of the isomerizing NA or whether it is also present in the dynamics of non-isomerizing pDNA. To address this question we will compare the transient IR spectra of pDNA with the above NA data.

3.2.3. Femtosecond IR spectroscopy of pDNA

In the pDNA measurements the same vibrational mode, namely the symmetric NO_2 stretch, as above will be focused on. For pDNA in DMSO-d_6 that mode is located at 1312 cm^{-1}, i.e. at a slightly lower frequency as in NA. Upon femtosecond excitation at 400 nm one observes the behavior detailed in Ref. [10] for the closely related molecule *para*-nitroaniline (Fig. 6a). Around time zero an

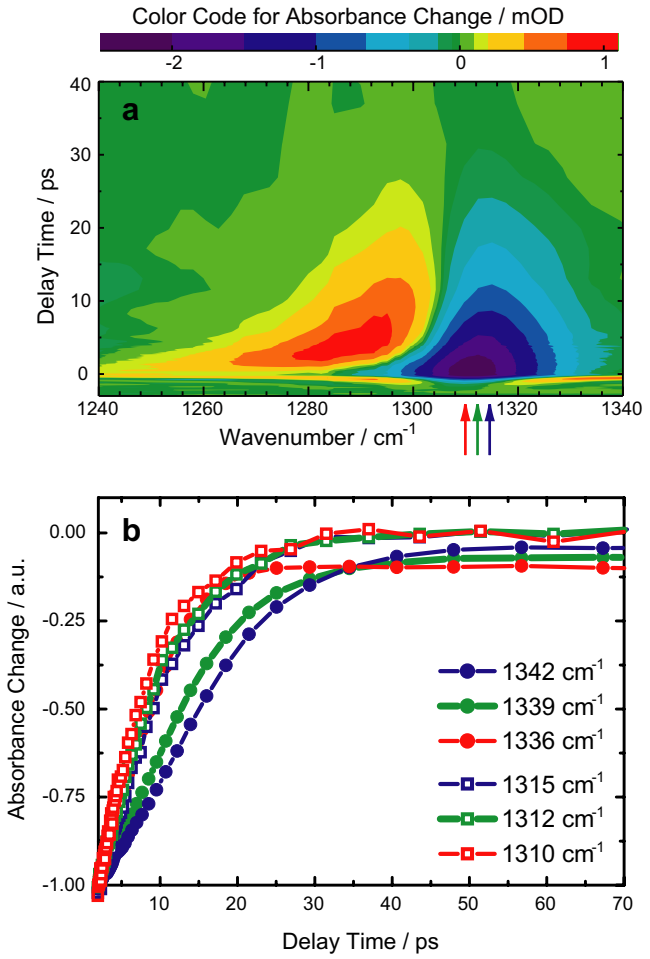

Fig. 6. Comparison of the femtosecond IR responses of pDNA and NA in the NO_2 stretch region. (a) Contour representation of the IR response of pDNA after 400 nm excitation. (b) Time traces for the bleach recovery of the NO_2 resonance. Red (green, blue) refers to the low (center, high) frequency part of the bleach spectrum. Filled symbols mark time trace of NA, open those of pDNA. (For interpretation of the references to color in this figure legend, the reader is referred to the web version of this article.)

intense bleach is seen due to the population of the electronically excited state. After internal conversion, i.e. after ~1 ps, an induced absorption adjacent to the low frequency edge of the bleach appears. Within some picoseconds the induced absorption peak moves to higher frequencies and concomitantly the bleach signal decreases. As outlined in Ref. [10] this decay correlates with vibrational cooling. The cooling dynamics could be retrieved from these data by the procedure used above for the Vis data. This approach works nicely for the pDNA data. Unfortunately, it cannot be adopted for NA. Here, the induced low frequency absorption of the NO_2 mode caused by the vibrational excitation is superimposed with the bleach of another mode (see Fig. 4a). This obstructs the determination of mean values of the absorption band. For the sake of direct comparison of the two molecules we thus have to use a different approach. We simply plot (normalized) IR time traces. Since a hallmark of vibrational cooling is a pronounced frequency dependence of

Table 2
Compiled results of single exponential fits of the IR data depicted in Fig. 6b

NA		pDNA	
$\tilde{\nu}$	τ_{ir}	$\tilde{\nu}$	τ_{ir}
1336	8	1310	7
1339	14	1312	9
1342	17	1315	10

The detection frequencies $\tilde{\nu}$ are given in cm^{-1}, the time constants τ_{ir} in picoseconds.

the time traces, one can already observe distinct differences between the time traces of one molecule (see Fig. 6b). Our approach for a realistic comparison is to follow the bleach signals of the NO_2 stretch modes at their center and their two spectral wings. We chose to normalize the traces at 2 ps since at that time internal conversion is terminated for either molecule. From Fig. 6b it is evident that for corresponding time traces, i.e. when comparing the two red wing traces, the two center traces and so on, the decay is also slower for NA. For the red (blue) edge the respective time constant differ by a factor of ~1.2 (1.7), for the central frequency the factor is ~1.6 (see compilation in Table 2). Moreover, the time traces of pDNA merge after 25 ps, whereas NA features frequency dependent decay patterns thereafter. Thus, the IR transients of NA are not only slower in comparison with their visible counterpart but also in comparison with the IR transients of pDNA.

4. Discussion

The experimental findings of this paper may be summarized as follows: The femtosecond signatures of the non-isomerizing molecule pDNA and the isomerizing molecule NA are very similar in the visible range. In either case a process on the 100 fs time scale is observed. For pDNA it has been associated with a NO_2 twist motion in the electronically excited state [4,7]. For NA the assignment is controversial. We have assigned this process to the motion of the excited molecule out of the Franck–Condon region [11]. Poprawa-Smoluch et al. [12] associate this process with a transition from the primarily excited $\pi\pi^*$ state to an $n\pi^*$ state. There is a consensus that the next kinetic step which takes ~1 ps in pDNA [7] and NA [11,12] describes the internal conversion to the ground state. The internal conversion is followed by the vibrational cooling of the ground state. Based on visible spectroscopy time constants of around 5 ps have been determined for this process. Again this applies for pDNA [7] and NA [11,12]. In particular, a direct comparison of the cooling signatures of pDNA and NA (see Fig. 2) affords a virtually identical behavior. In sharp contrast to this matching behavior of the visible transients distinct deviations are observed in the IR. These are pronounced after the internal conversion. The recovery of the bleach of the NO_2 stretch vibration takes roughly a factor of 1.6 longer for NA as compared

to pDNA. Further there are spectral changes with a small amplitude with even longer characteristic times (Fig. 6b).

From these findings two questions arise. (i) Why do certain processes not leave a signature in the visible spectroscopy? (ii) What is the nature of these processes? Definitely when addressing these two questions we can focus on the nuclear degrees of freedoms of the NA molecule (and maybe its solvent surroundings) since the electronic excitation decays on much shorter time scales. Thus, we are looking for structural changes of NA in its electronic ground state that do not have an impact on its visible absorption spectrum.

(i) Spectroscopy textbooks (e.g. Ref. [20]) tell us that a displacement Δ_v along a certain mode upon excitation (Franck–Condon active mode) is a prerequisite for an influence on the shape of visible absorption spectra. For larger molecules in solution with their structureless absorption bands an assignment of the Franck–Condon active modes based on the absorption spectrum is not feasible. However, a resonance Raman experiment can afford those modes [21,22]. A thorough analysis of the resonance Raman spectrum of NA performed by Biswas and Umapathy [23] yielded in addition to a low frequency solvent contribution eight vibrational modes (out of 96) that contribute to the absorption spectrum of NA. These modes all lie in a range between 1100 and 1600 cm^{-1} whereby the symmetric NO_2 stretch mode shows the strongest contribution. It is that very vibrational mode for which the slow kinetics in the IR experiments have a strong amplitude. One might now argue that the modulation of this strongly Franck–Condon active mode should have an impact on the visible absorption spectrum and therefore the slow process should be present in the UV/Vis experiment. Yet, the slow process mainly effects the amplitude of the IR signal and only to a minor extent its frequency ω_v (see Fig. 4). The resonance Raman intensity and thereby the Franck–Condon factor for a mode v is proportional to $\Delta_v^2\omega_v^2$ [21,23]. If ω_v is constant during a process a change in the amplitude of an IR resonance need not modulate the electronic absorption spectrum (provided that the displacement Δ_v remains constant too.) Thus, we are dealing with a process that modulates the IR absorption of a vibrational resonance, i.e. its oscillator strength, and not its eigen frequency. Indeed as the difference spectra in Fig. 3 demonstrate, strong structural changes like the *trans* → *cis* isomerization affect only the vibrational oscillator strength and not the resonance frequency of the NO_2 stretch mode. In other words, this mode seems to "sense" structural changes via its oscillator strength and not via its frequency. As this frequency (and that of other high frequency modes) remains virtually constant during the slow process, the visible spectrum is not modulated by this process.

(ii) So what is the nature of this process? Two experimental observations might give a clue. First, the quantum yield of the isomerization is rather low (~10%). Second, the IR difference spectra after 20–30 ps resemble a scaled up cw *cis–trans* difference spectrum. Based on these observations a preliminary model for the slow process is developed (cf. Fig. 7). Photo-excitation of the *trans*-isomer promotes the molecule to an electronically excited state. There the altered potential generates forces which result in a motion out of the Franck–Condon region towards a transition region to the ground state. We postulate that the structure the molecule adopts in the transition region is closer to that of the *cis*-form than that of the *trans*-form. At the transition region a branching occurs. A minor fraction of molecules form the *cis*-isomer, the remainder takes a route which ultimately leads back to the *trans*-isomer. Along this route a shallow minimum exists in which some fraction of the population is intermediately trapped. The molecules leave that shallow trap in the time scale of 10 ps. As this process does not show up in the visible spectroscopy the molecule experiences the barrier along Franck–Condon-inactive modes. Along these modes the trap structure is closer to that of the *cis*-isomer (*cisoid* in Fig. 7) which is why a scaled up cw difference spectrum is observed. When comparing the DFT structures of *trans*- and *cis*-NA (see Fig. 7) it becomes evident that distortions of many internal degrees of freedom (vibrational modes) are necessary to re-transform the *cis* isomer into the *trans* form. Several of them will be Franck–Condon inactive and their evolution is only observed in the IR via anharmonic couplings. In short, we attribute the slow process to dynamics in the ground state surface which is rough along Franck–Condon-inactive modes.

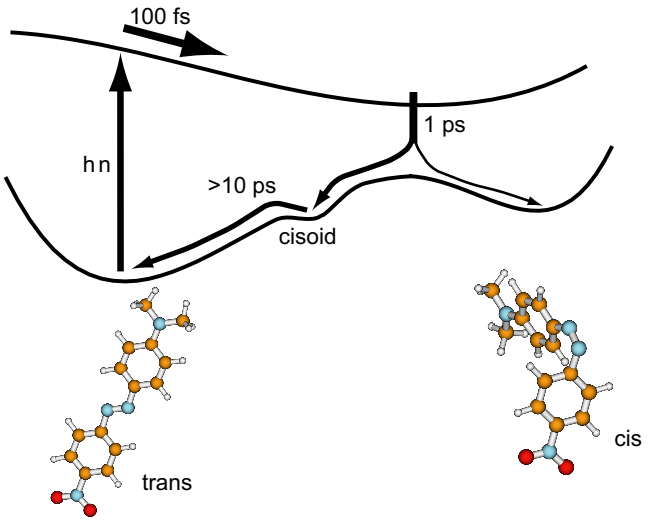

Fig. 7. Schematic of the proposed model on the photo-isomerization of NA. For simplicity cooling processes also taking place have been omitted. The depicted structures of *trans* and *cis* NA resulted from a DFT calculation.

5. Conclusions

In this study we have monitored an ultrafast photo-isomerization of an azo-dye by two femtosecond probing schemes, visible and IR spectroscopy. By visible spectroscopy signatures of expected processes as there are motion in or between excited states, internal conversion to the

ground state, and vibrational cooling are observed. Maybe due to a limited time resolution IR probing misses the excited state motion occurring with a characteristic time of ~100 fs. The internal conversion takes about 1 ps and is seen by both techniques. The same applies to ground state cooling which is terminated in roughly 10 ps. To our surprise in the IR pronounced changes lasting until ~50 ps are detected. These changes find no counterpart in the visible experiment. Presently, we associate these changes with smaller re-organizations that take the nascent azo-dye from the structure adopted immediately after internal conversion to the relaxed forms of the isomers. It seems that these re-organizations mainly involve Franck–Condon silent modes. It would be of great interest to see whether such a discrepancy between visible and IR observables is observed for other isomerizing molecules too.

Acknowledgments

This work was supported by Deutsche Forschungsgemeinschaft through the DFG-Cluster of Excellence Munich-Centre for Advanced Photonics and through the Sonderforschungsbereich (SFB) 533. T. Cordes is grateful for a scholarship donated by the Fonds der chemischen Industrie. We thank W. Zinth for very helpful discussion and continuous support of this work.

References

[1] N. Tamai, H. Miyasaka, Chem. Rev. 100 (2000) 1875.
[2] E. Lenderink, K. Duppen, D.A. Wiersma, J. Phys. Chem. 99 (1995) 8972.
[3] K. Gille, H. Knoll, K. Quitzsch, Int. J. Chem. Kinet. 31 (1999) 337.
[4] V.M. Farztdinov, R. Schanz, S.A. Kovalenko, N.P. Ernsting, J. Phys. Chem. A 104 (2000) 11486.
[5] C.L. Thomsen, J. Thømsen, S.R. Keiding, J. Phys. Chem. A 102 (1998) 1062.
[6] S.A. Kovalenko, R. Schanz, V.M. Farztdinov, H. Hennig, N.P. Ernsting, Chem. Phys. Lett. 323 (2000) 312.
[7] S.A. Kovalenko, S. Schanz, H. Hennig, N.P. Ernsting, J. Chem. Phys. 115 (2001) 3256.
[8] V. Kozich, W. Werncke, J. Dreyer, K.W. Brzezinka, M. Rini, A. Kummrow, T. Elsaesser, J. Chem. Phys. 117 (2002) 719.
[9] Q. An, P. Gilch, Chem. Phys. Lett. 363 (2002) 397.
[10] T. Schrader, A. Sieg, F. Koller, W. Schreier, Q. An, W. Zinth, P. Gilch, Chem. Phys. Lett. 392 (2004) 358.
[11] B. Schmidt, C. Sobotta, S. Malkmus, S. Laimgruber, M. Braun, W. Zinth, P. Gilch, J. Phys. Chem. A 108 (2004) 4399.
[12] M. Poprawa-Smoluch, J. Baggerman, H. Zhang, H.P.A. Maas, L. De Cola, A.M. Brouwer, J. Phys. Chem. A 110 (2006) 11926.
[13] T. Cordes, D. Weinrich, S. Kempa, K. Riesselmann, S. Herre, C. Hoppmann, K. Rück-Braun, W. Zinth, Chem. Phys. Lett. 428 (2006) 167.
[14] M.J. Frisch et al. Gaussian 98, Revision A.7.
[15] A. Seilmeier, W. Kaiser, in: W. Kaiser (Ed.), Topics in Applied Physics, vol. 60, Elsevier, Amsterdam, 1993, p. 279 (Chapter 7).
[16] N. Biswas, S. Umapathy, J. Phys. Chem. A 104 (2000) 2734.
[17] C.H.B. Cruz, P.C. Becker, J.P. Gordon, R.L. Fork, C.V. Shank, IEEE J. Quantum Electron. 24 (1988) 261.
[18] P. Hamm, Chem. Phys. 200 (1995) 415.
[19] K. Wynne, R.M. Hochstrasser, Chem. Phys. 193 (1995) 211.
[20] J.M. Hollas, Modern Spectroscopy, fourth ed., Wiley, Chichester, 2003.
[21] A.B. Myers, Chem. Rev. 96 (1996) 911.
[22] A.B. Myers, Annu. Rev. Phys. Chem. 49 (1998) 267.
[23] N. Biswas, S. Umapathy, J. Raman Spectrosc. 32 (2001) 471.